Results in Physics 9 (2018) 897–903

Contents lists available at ScienceDirect

Results in Physics

journal homepage: www.elsevier.com/locate/rinp

The effects of Poynting–Robertson drag on solar sails

F.A. Abd El-Salam[a,b,*]

[a] Department of Mathematics, Faculty of Science, Taibah University, Al-Madinah, Saudi Arabia
[b] Department of Astronomy, Faculty of Science, Cairo University, Cairo 12613, Egypt

ARTICLE INFO

Keywords:
Poynting–Robertson drag
Solar sail
Control laws
Optimal sail
Cone angle

ABSTRACT

In the present work, the concept of solar sailing and its developing spacecraft are presented. The effects of Poynting–Robertson drag on solar sails are considered. Some analytical control laws with some mentioned input constraints for optimizing solar sails dynamics in heliocentric orbit using Lagrange's planetary equations are obtained. Optimum force vector in a required direction is maximized by deriving optimal sail cone angle. New control laws that maximize thrust to obtain certain required maximization in some particular orbital element are obtained.

Introduction

The theoretical concept of solar sails is old-standing and dates back to Kepler when he observed that comet tails point away from the Sun and suggested that the Sun caused the effect. Solar sails are form of spacecraft propulsion using a combination of light (radiation pressure) and high speed ejected gasses from a star (e.g. solar wind and coronal mass ejection) to push large ultra-thin mirrors to high speeds. This was first introduced in the 1920s by the father of Russian astronautics, Tsiolkovsky [1] and Tsander [2]. It is also used in the spacecraft attitude dynamics, Rizvi [3], he developed a control method for the solar sail normal vector to trace a desired circular coning trajectory at orbit rate. He finally concludes that the control torques can be applied to the sailcraft to enable orbit rate cone tracing of the sail normal and yield the desired orbital effects. Wright [4] presented a detailed analysis on some possible solar sail applications. During his time at the Jet Propulsion Laboratory (JPL), Wright was actively involved in the planning of a rendezvous mission to comet Halley using solar sail technology, but solar electric propulsion concept was selected instead, primarily because of technology maturity. Not long thereafter, this mission was dropped by NASA.

The sail concept is performed by gaining momentum from an ambient source, Solar Electromagnetic Radiation. Using momentum gained only by reflecting ambient sunlight, the sail is slowly but continuously accelerated to accomplish a wide-range of potential missions. Light sails could also be driven by energy beams to extend their range of operations, which is strictly beam sailing rather than solar sailing. Solar sails offer the possibility of low-cost operations combined with long operating lifetimes. Since they have few moving parts and use no propellant, they can potentially be used numerous times for delivery of payloads. The mechanism of this concept refer to the momentum carried by individual photons is extremely small. Thus, to provide a suitably large momentum transfer we require the sail to have a large surface, while maintaining as low a mass as possible. At best a solar sail will experience a pressure about 9 N/km^2 located in Earth orbit. Adding the impulse due to incident and reflected photons it is found that the thrust vector is directed normal to the surface of the sail, hence by controlling the orientation of the sail relative to the Sun we can gain or lose orbital angular momentum.

The literature on sailing dynamics, development and its attitude control is wealth and it is of great interest to sketch some important ideas on these problems. The first solar sail trajectories were calculated by Tsu [5] and London [6]. Tsu investigated various means of propulsion and showed that in many cases solar sails show superior performance when compared to chemical and ion propulsion systems. He used approximated heliocentric equations of motion to obtain spiraling trajectories. London presented similar spiral solutions for Earth-Mars transfers with constant sail orientation using the exact equations of motion. Optimal solar sail trajectories were first computed by Zhukov and Lebedev [7] for interplanetary missions between coplanar circular orbits. In 1980 Jayaraman [8] published similar minimum-time trajectories for transfers between the Earth and Mars. Two years later, Wood et al. [9] presented an analytical proof to show that the orbital transfer times obtained by Jayaraman [8] were incorrect due to the incorrect application of a transversality condition of variational calculus and an erroneous control law. Powers et al. [10] and Powers and Coverstone [11] obtained results similar to those reported in Wood's paper, and obtained solutions for transfers to synchronous orbits. The

* Address: Department of Mathematics, Faculty of Science, Taibah University, Al-Madinah, Saudi Arabia.
E-mail address: f.a.abdelsalam@gmail.com.

https://doi.org/10.1016/j.rinp.2018.03.057
Received 28 December 2017; Received in revised form 16 March 2018; Accepted 27 March 2018
Available online 31 March 2018

more general time-optimal control problem of three-dimensional, inclined and elliptic departure and rendezvous planet orbits was discussed by Sauer [12]. Hughes and McInnes [13] used Genetic Algorithms and Sequential Quadratic Programming to obtain interplanetary trajectories via a direct method. Dachwald [14] presented a novel approach based on Evolutionary Neuro-controllers (ENC) to calculate optimal solar sail trajectories for interplanetary missions. Thomas, et al. [15] considered the orbital dynamics of a solar sail in the Earth-Sun circular restricted 3-body problem. They found there are equilibria admitting homoclinic paths where the stable and unstable invariant manifolds are identical. Bong Wie [16] developed an attitude control systems for solar sail spacecraft are presented. He analysed a sailcraft in an Earth centered elliptic orbit, with particular emphasis on the significant effect of a solar-pressure disturbance torque (caused by an uncertain center-of-mass and center-of-pressure offset).

Sheng-Ping Gong et al. [17] investigated the time-optimal interplanetary transfer trajectories to a circular orbit of given inclination and radius. They derived optimal control law from the principle of maximization. An indirect method is used to solve the optimal control problem by selecting values for the initial adjoint variables. In contrast to ordinary ballistic navigation the mission analysis for solar sail trajectories is not a simple task. The difference is that ballistic navigation is determined by a finite sequence of maneuvers, each of them being fully defined by a Keplerian theory. But solar sailing, on the contrary, is a continuous process and the mathematics for reaching final conditions is far more complex, even more than in the case of electric propulsion, since the thrust intensity is related to the sail orientation: the orientation of the force vector applying to a perfectly reflective solar sail is normal to the sail, in the anti-solar direction. Its intensity is proportional to the square cosine of the angle between the normal to the sail and the Sun-line. Abd El-Salam [18] treated the effects of direct solar radiation pressure, the force due to coronal mass ejections and solar wind on the sailcraft configurations. He obtained some new analytical control laws with some mentioned input constraints for optimizing sailcraft dynamics in heliocentric orbit using Lagrange's planetary equations are obtained. In the present work the author aims to tackle the additional perturbing effect called the Poynting–Robertson drag on solar sails.

IKAROS and LightSail

In May 2010, "a mission to Venus with a secondary payload called Interplanetary Kite-craft Accelerated by Radiation of the Sun (IKAROS) was launched by "JAXA" the Japan Aerospace Exploration Agency. JAXA proposed a concept of "Solar Power Sail" for future deep space exploration [19,20]. It combines the concept of solar sail (photon propulsion) with a larger power generation by flexible solar cells attached on the sail membrane. IKAROS successfully deployed a 20 m-span sail on June 9, and then performed an interplanetary solar-sailing taking, see for more details Tsuda et al. [21].

LightSail1,2 (LS1,2) is a flagship program of The Planetary Society (TPS), The LS1 mission served as an important engineering pathfinder for the goal of demonstrating solar sailing in LEO. LS1 is successfully completed its mission in low Earth orbit during spring 2015, and the LS2 mission is scheduled for launch in 2017. See for more details; Spencer et al. [22], Betts, et al. [23,24], Hilverda and Davis [25] and Plante, et al. [26].

The Poynting–Robertson drag

Light exerts a small drag force on small dust particles. For large or reflective bodies, radiation pushes on objects very slightly. However, for very small particles (in size, not mass) in orbit around a star, radiation slows the particles, causing them to gradually spiral inwards. This effect was first discovered by Poynting in [27] and later derived rigorously by Robertson [28] in 1937. The Poynting–Robertson force is given by

$$\mathbf{F}_{PR} = -\frac{W}{c^2}\mathbf{v} \tag{1}$$

where $\mathbf{v}$, W, c are the grain's velocity, the power of the incoming radiation of the Sun and the speed of light respectively. Let the Sun's energy flux be given by the Poynting vector $\boldsymbol{S}$ ($\boldsymbol{S}$ represents the directional energy flux density (the rate of energy transfer per unit area, in units of watts per square meter) of an electromagnetic field. Let the dust particle have a cross sectional area A and be perfectly absorbing, then the energy absorbed by the dust particle per unit time $W = PA$ is the power, where $P = 4.563 \times 10^{-6}\,\mathrm{N/m^2}$ is the nominal solar-radiation pressure constant at 1 AU from the Sun. If the particle is moving at speed v relative to the Sun then the Poynting vector $\boldsymbol{S}$ must be corrected by $\boldsymbol{S}(1-\dot{r}/c)$ where $\dot{r} = \mathbf{v}\cdot\hat{\boldsymbol{S}}$ is the radial velocity of the particle away from the Sun. The momentum removed per second from the Sun's rays, by the dust particle, is $\boldsymbol{S}(1-\dot{r}/c)A/c$ which is the radiation pressure force. The absorbed energy flux is re-radiated by the particle. In the rest frame of the particle, the radiation emitted is almost isotropic so there is no net force on the particle in its own rest frame. However, the re-radiation is equivalent to an energy loss rate $\boldsymbol{S}(1-\dot{r}/c)A/c^2$, which has velocity $\mathbf{v}$ when viewed from the rest frame of the Sun. In the solar rest frame, the particle has a drag force of $-S(1-\dot{r}/c)A\mathbf{v}/c^2$. Since the dust particle is losing momentum, while its mass is conserved, the particle is decelerated. The momentum loss per unit time is

$$\begin{aligned} m\dot{\mathbf{v}} &= \boldsymbol{S}(1-\dot{r}/c)A/c - SA\mathbf{v}/c^2 \\ &= \tfrac{PA}{c}(\hat{\boldsymbol{S}}(1-\dot{r}/c)-\mathbf{v}/c) \end{aligned} \tag{2}$$

Comparison of this equation with that given by Klacka et al. [29] Eq. (21) there, reflects that the pressure in my notations is given in terms of his notation by $P = SQ'_{pr}$ where S solar energy flux density and Q'_{pr} is the stellar spectrum.

The last term on the right is the Poynting–Robertson drag and equivalent to the Robertson result. Historically, this form of radiation reaction was first developed by Abraham [30] for an electron. Similar force terms arise in the relativistic LAD (Lorentz, Abraham and Dirac) equation see, Dirac [31], Pauli's book [32] and Lorentz [33], who quotes Abraham's result

$$\mathbf{F}_{PR} = \frac{PA}{c}(\mathbf{v}/c) = \frac{PA}{c^2}\mathbf{v} = \frac{r^2 L_s}{4c^2}\sqrt{\frac{GM_s}{R^5}}\,\hat{\mathbf{v}} \tag{3}$$

where G, R, M_s, L_s, r_g are the universal gravitational constant, the grain's orbital radius, the mass, the luminosity of the Sun and the grain's radius respectively. The PR effect is also stronger closer to the Sun. Gravity varies as R^{-2} whereas the PR force varies as $R^{-2.5}$, so the effect also gets relatively stronger as the object approaches the Sun. This tends to reduce the eccentricity of the object's orbit in addition to dragging it in. Thus the only component of PR effects in STW coordinate system is given by

$$\mathbf{F}_{PR} = -\frac{r^2 L_s}{4c^2}\sqrt{\frac{GM_s}{R^5}}\,\hat{\mathbf{e}}_s = -\frac{r^2 L_s}{4c^2}\sqrt{\frac{GM_s}{R^5}}\,(\cos\alpha\,\hat{\mathbf{n}} + \sin\alpha\,\hat{\mathbf{t}}) \tag{4}$$

The $\hat{\mathbf{t}}$-component give no contribution to the thrust vector, thus

$$\mathbf{F}_{PR} = -\frac{r^2 L_s}{4c^2}\sqrt{\frac{GM_s}{R^5}}\,(\cos^2\alpha\,\hat{\mathbf{e}}_s + \cos\alpha\sin\alpha\cos\delta\,\hat{\mathbf{e}}_t + \cos\alpha\sin\alpha\sin\delta\,\hat{\mathbf{e}}_w) \tag{5}$$

where α and δ are the sail control angles defined as depicted in the Fig. 1.

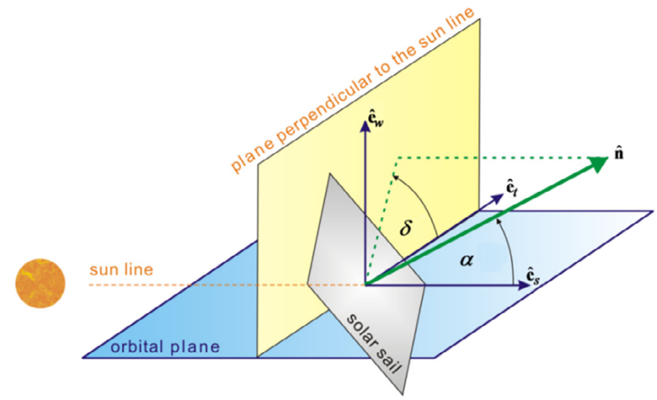

Fig. 1. Definition of sail control angles.

Optimum force vector

The force model due to the PR drag is given by

$$\mathbf{F}_{PR} = -\frac{r^2 L_s}{4c^2}\sqrt{\frac{GM_s}{R^5}}\left(\cos^2\alpha\,\mathbf{e}_s + \cos\alpha\sin\alpha\cos\delta\,\mathbf{e}_t + \cos\alpha\sin\alpha\sin\delta\,\mathbf{e}_w\right) \tag{6}$$

Referring to Fig. 1, we see the orientation of the solar sail, and so the thrust force vector, is described relative to the Sun-line by the sail pitch angle, α, and clock angle, δ. We note that the sail control angles α, δ can be defined as either;

$$0^\circ < \alpha < 90^\circ, \quad 0^\circ < \delta < 360^\circ \quad \text{or} \quad -90^\circ < \alpha < 0^\circ, \quad 0^\circ < \delta < 360^\circ$$

Now, the sail thrust vector is defined by the cone and clock angles in the radial-transverse-normal (STW) frame. In order to optimize the sail control angles, we define a required direction, $\hat{\xi}$ along which the component of the sail thrust is to be maximized,

$$\hat{\xi} = \cos\tilde{\alpha}\,\hat{\mathbf{e}}_s + \sin\tilde{\alpha}\cos\tilde{\delta}\,\hat{\mathbf{e}}_t + \sin\tilde{\alpha}\sin\tilde{\delta}\,\hat{\mathbf{e}}_w \tag{7}$$

The force in this required direction, namely $\hat{\xi}$-direction;

$$F_\xi = \mathbf{F}\cdot\hat{\xi} = -\frac{r^2 L_s}{4c^2}\sqrt{\frac{GM_s}{R^5}}\cos^2\alpha(\mathbf{e}_s\cdot\hat{\xi}) - \frac{r^2 L_s}{4c^2}\sqrt{\frac{GM_s}{R^5}}\cos\alpha\sin\alpha\cos\delta(\mathbf{e}_t\cdot\hat{\xi}) - \frac{r^2 L_s}{4c^2}\sqrt{\frac{GM_s}{R^5}}\cos\alpha\sin\alpha\sin\delta(\mathbf{e}_w\cdot\hat{\xi}) \tag{8}$$

which can be rewritten as

$$F_\xi = -\frac{r^2 L_s}{4c^2}\sqrt{\frac{GM_s}{R^5}}\left(\cos^2\alpha\cos\tilde{\alpha} + \cos\alpha\sin\alpha\cos\delta\sin\tilde{\alpha}\cos\tilde{\delta} + \cos\alpha\sin\alpha\sin\delta\sin\tilde{\alpha}\sin\tilde{\delta}\right) \tag{9}$$

Arranging terms and using the trigonometric identities we get

$$F_\xi = \mathscr{A}_{PR}\left[\cos^2\alpha\cos\tilde{\alpha} + \cos\alpha\sin\alpha\sin\tilde{\alpha}\cos(\delta-\tilde{\delta})\right] \tag{10}$$

where

$$\mathscr{A}_{PR} = -\frac{r^2 L_s}{4c^2}\sqrt{\frac{GM_s}{R^5}}$$

Eq. (10) can be simplified to

$$F_\xi = \mathscr{A}_0\cos^2\alpha\cos\tilde{\alpha} + \mathscr{A}_1\cos\alpha\cos\tilde{\alpha} + \mathscr{A}_2(\cos\alpha\cos\tilde{\alpha} + \sin\alpha\sin\tilde{\alpha}\cos(\delta-\tilde{\delta}))\cos^2\alpha + \mathscr{A}_3\cos\alpha\sin\alpha\sin\tilde{\alpha}\cos(\delta-\tilde{\delta}) \tag{11}$$

Differentiating Eq. (11) with respect to the cone angle and find the turning points, $(\partial F_\xi/\partial\alpha)$, then we can obtain the optimal sail cone angle, which maximizes the force in the required direction as

$$\frac{\partial F_\xi}{\partial\alpha} = 0 = -2\mathscr{A}_{PR}\left\{\cos\alpha\sin\alpha\cos\tilde{\alpha} + \frac{1}{2}[\cos^2\alpha-\sin^2\alpha]\sin\tilde{\alpha}\cos(\delta-\tilde{\delta})\right\} = 0$$

Dividing on $3\cos^2\alpha\sin\alpha$ yields

$$-\frac{1}{3}\mathscr{A}_{PR}\left\{2\sec\alpha\cos\tilde{\alpha} - \frac{1}{\sin\alpha}[(1-\tan^2\alpha)]\sin\tilde{\alpha}\cos(\delta-\tilde{\delta})\right\} = 0$$

$$-\frac{1}{3}\mathscr{A}_{PR}\left\{2\sec\alpha\cos\tilde{\alpha} + \frac{1}{\sin\alpha}\sin\tilde{\alpha}\cos(\delta-\tilde{\delta}) - \frac{1}{\sin\alpha}\tan^2\alpha\sin\tilde{\alpha}\cos(\delta-\tilde{\delta})\right\} = 0$$

Which can be simplified to

$$\left(\frac{\mathscr{A}_{PR}}{3\cos\alpha\sin\alpha}\right)\{-2\cos\tilde{\alpha}\sin\alpha + \sin\tilde{\alpha}\cos(\delta-\tilde{\delta})\cos\alpha - \tan^2\alpha\sin\alpha\sin\tilde{\alpha}\cos(\delta-\tilde{\delta})\} = 0$$

Equating the numerator to zero and rearranging the terms yields

$$2\cos\tilde{\alpha}\sin\alpha - \sin\tilde{\alpha}\cos(\delta-\tilde{\delta})\cos\alpha + \sin\tilde{\alpha}\cos(\delta-\tilde{\delta})\tan^2\alpha\sin\alpha = 0$$

Dividing on $\cos\alpha$ yields

$$\sin\tilde{\alpha}\cos(\delta-\tilde{\delta})\tan^3\alpha + 2\cos\tilde{\alpha}\tan\alpha - \sin\tilde{\alpha}\cos(\delta-\tilde{\delta}) = 0$$

This equation has only one real solution and the other two are complex, then the real one in the maximizing $\alpha = \alpha^*$ direction ξ is given by

$$\tan\alpha^* = \sqrt[3]{\frac{1}{2}\tan\tilde{\alpha} + \sqrt{\frac{1}{2}\tan^2\tilde{\alpha} + \frac{8}{27}\cot^3\tilde{\alpha}\sec^3(\delta-\tilde{\delta})}} \tag{12}$$

Lagrange's planetary equations

The state of a spacecraft can be described by a vector of 6 orbital elements, namely semi-major axis, a, eccentricity, e, inclination, i, argument of perihelion, ω, right ascension of the ascending node, Ω, true anomaly, f or any other time element. Theses 6 elements are equivalent to 6 Cartesian position and velocity components. To measure the rate of change in these elements, we use the very famous system of 6 first order differential equations known as Lagrange planetary equations see Eqs. (13)–(18). They are used to solve the equations of motion of the sail. These equations are particularly useful when we want to maximize the rate of change of a particular orbital element. This is useful when we want to modify one orbital element, while leaving the other time-averaged elements unchanged. One form of this system is given by

$$\frac{da}{df} = \frac{2pr^2}{\mu(1-e^2)^2}\left[S e\sin f + T\frac{p}{r}\right] \tag{13}$$

$$\frac{de}{df} = \frac{r^2}{\mu}\left[S\sin f + T\left(1+\frac{r}{p}\right)\cos f + T\frac{r}{p}e\right] \tag{14}$$

$$\frac{di}{df} = \frac{r^3}{\mu p}\cos(f+\omega)W \tag{15}$$

$$\frac{d\Omega}{df} = \frac{r^3}{\mu p\sin i}\sin(f+\omega)W \tag{16}$$

$$\frac{d\omega}{df} = -\frac{d\Omega}{df}\cos i + \frac{r^2}{\mu e}\left[-S\cos f + T\left(1+\frac{r}{p}\right)\sin f\right] \tag{17}$$

$$\frac{dt}{df} = \frac{r^2}{\sqrt{\mu p}}\left[1 - \frac{r^2}{\mu e}\left[S\cos f - T\left(1+\frac{r}{p}\right)\sin f\right]\right] \tag{18}$$

where a, e, i, Ω, ω, f are the usual Keplerian orbital elements, p is the semi-latus rectum, μ the gravitational parameter, and n is the orbital mean motion. The components of the solar sail thrust are denoted by S, T, W radial, transverse, and normal respectively. All Lagrange planetary equations can be written in a compact form in only one equation as an inner product of a force vector and a primer vector of optimization;

$$\frac{d\mathscr{X}}{df} = \boldsymbol{F}\cdot\Xi^{\mathscr{X}} \tag{19}$$

where $\mathscr{X}(\equiv a, e, i, \Omega, \omega, f)$ denotes any element of the Keplerian orbital elements. $\boldsymbol{F}$, $\Xi^{\mathscr{X}}$ are the force vector and primer vector of optimization respectively. These vectors can be conveniently written as;

$$\boldsymbol{F} = S\,\hat{\mathbf{e}}_s + T\,\hat{\mathbf{e}}_t + W\,\hat{\mathbf{e}}_w \quad \text{and} \quad \Xi^{\mathscr{X}} = \Xi_s^{\mathscr{X}}\,\hat{\mathbf{e}}_s + \Xi_t^{\mathscr{X}}\,\hat{\mathbf{e}}_t + \Xi_w^{\mathscr{X}}\,\hat{\mathbf{e}}_w$$

where

$$S = -\frac{r^2 L_s}{4c^2}\sqrt{\frac{GM_s}{R^5}}\cos^2\alpha \tag{20}$$

$$T = -\frac{r^2 L_s}{4c^2}\sqrt{\frac{GM_s}{R^5}}\cos\alpha\sin\alpha\cos\delta \tag{21}$$

$$W = -\frac{r^2 L_s}{4c^2}\sqrt{\frac{GM_s}{R^5}}\cos\alpha\sin\alpha\sin\delta \tag{22}$$

The primer vector in the direction of maximizing the semi-major axis is

$$\Xi^a = \Xi_S^a\hat{\mathbf{e}}_S + \Xi_t^a\hat{\mathbf{e}}_t = \frac{2pr^2}{\mu(1-e^2)^2}\left[e\sin f\,\hat{\mathbf{e}}_s + \frac{p}{r}\hat{\mathbf{e}}_t\right] \tag{23}$$

the primer vector in the direction of maximizing the eccentricity is

$$\Xi^e = \Xi_s^e\hat{\mathbf{e}}_s + \Xi_t^e\hat{\mathbf{e}}_t = \frac{r^2}{\mu}\left[\sin f\,\hat{\mathbf{e}}_S + \left(1 + \frac{r}{p}(e + \cos f)\right)\hat{\mathbf{e}}_t\right] \tag{24}$$

the primer vector in the direction of maximizing the inclination is

$$\Xi^i = \Xi_w^i\hat{\mathbf{e}}_w = \frac{r^2}{\mu P}\cos(f+\omega)\,\hat{\mathbf{e}}_w, \tag{25}$$

the primer vector in the direction of maximizing the longitude of the ascending node is

$$\Xi^\Omega = \Xi_w^\Omega\hat{\mathbf{e}}_w = \frac{r^2}{\mu P\sin i}\sin(f+\omega)\,\hat{\mathbf{e}}_w, \tag{26}$$

the primer vector in the direction of maximizing the argument of periapsis is

$$\Xi^\omega = \Xi_s^\omega\hat{\mathbf{e}}_s + \Xi_t^\omega\hat{\mathbf{e}}_t + \Xi_w^\omega\hat{\mathbf{e}}_w = \frac{r^2}{\mu e}\left[-\frac{er}{p\sin i}\sin(f+\omega)\cos i\,\hat{\mathbf{e}}_s - \cos f\,\hat{\mathbf{e}}_t + \left(1 + \frac{r}{p}\right)\sin f\,\hat{\mathbf{e}}_w\right], \tag{27}$$

Using this system we can maximize directly any orbital elements or any other dynamical orbital parameter such as, the radius of periapsis and apoapsis. For example, if the radius of apoapsis, $r_A = a(1+e)$ is differentiated, we obtain

$$\frac{dr_A}{df} = \frac{da}{df}(1+e) + a\frac{de}{df}.$$

Some new locally optimal control laws

To maximize the thrust to obtain certain required maximization in some particular orbital element we set $\frac{\partial}{\partial\alpha}\left(\frac{d\mathscr{X}}{df}\right) = 0$ and thus obtain a new set of locally optimal control laws. These control laws cannot guarantee global optimality, and they are often termed closed loop methods. Global optimality requires the use of numerical methods, and even then, the true optimum solution is hard to attain.

Optimal control law for the rate of change of semi-major axis

The primer vector components maximize the first Lagrange planetary equation for the rate of change of semi-major axis. In what follows we will find an optimum cone angle that maximize the rate of change of semi-major axis

$$\frac{\partial}{\partial\alpha}\left(\frac{da}{df}\right) = \frac{2pr^2}{\mu(1-e^2)^2}\left[e\sin f\left(\frac{\partial S}{\partial\alpha}\right) + \frac{p}{r}\left(\frac{\partial T}{\partial\alpha}\right)\right] = 0 \Rightarrow \left[e\sin f\left(\frac{\partial S}{\partial\alpha}\right) + \frac{p}{r}\left(\frac{\partial T}{\partial\alpha}\right)\right] = 0$$

The force in this required direction is given by.

$$\frac{da}{dt} = \mathbf{F}\cdot\Xi^a = P\frac{2pr^2}{\mu(1-e^2)^2}\left\{e\sin f\left[-\frac{r^2L_s}{4c^2}\sqrt{\frac{GM_s}{R^5}}\cos^2\alpha\right] - \frac{p}{r}\left[\frac{r^2L_s}{4c^2}\sqrt{\frac{GM_s}{R^5}}\cos\alpha\sin\alpha\cos\delta\right]\right\} \tag{28}$$

Eq. (28) can be simplified to

$$\frac{da}{dt} = \frac{2r_g^2L_spr^2P}{\mu 4c^2(1-e^2)^2}\sqrt{\frac{GM_s}{R^5}}\left\{-e\sin f\cos^2\alpha - \frac{p}{r}[\cos\alpha\sin\alpha\cos\delta]\right\} \tag{29}$$

differentiating Eq. (29) with respect to the cone angle and find the turning points yields

$$\frac{\partial}{\partial\alpha}\left(\frac{da}{dt}\right) = 0 = \frac{2r_g^2L_spr^2P}{\mu 4c^2(1-e^2)^2}\sqrt{\frac{GM_s}{R^5}}\left\{2e\sin f\cos\alpha\sin\alpha + \frac{p}{r}[\cos^2\alpha - \sin^2\alpha]\cos\delta\right\} \tag{30}$$

The zeros of this equation gives the optimal sail cone angle, which maximizes the force in the required direction. Eq. (30) is a transcendental equation which is so difficult to be solved analytically, but in following we will consider some special cases (Figs. 2.1 and 2.2).

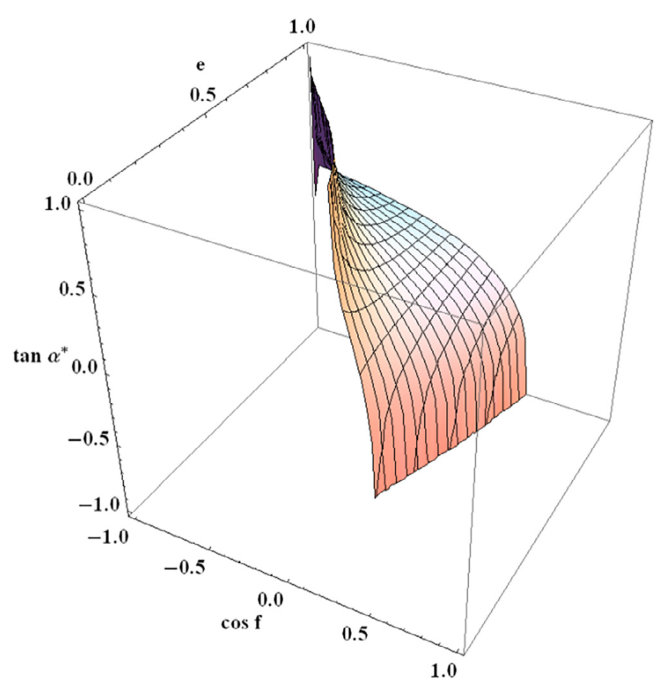

Fig. 2.1. The optimum cone angle that maximize the rate of change of semi-major axis when taking the positive sign in the numerator.

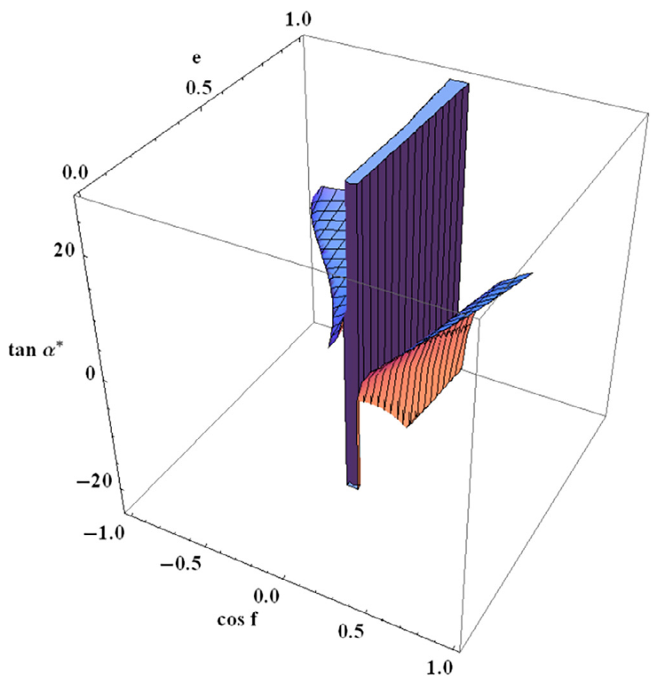

Fig. 2.2. The optimum cone angle that maximize the rate of change of semi-major axis when taking the negative sign in the numerator.

$$2e\sin f\cos\alpha\sin\alpha + \frac{1+e\cos f}{e\sin f}[\cos^2\alpha - \sin^2\alpha]\cos\delta = 0$$

$$2e^2\sin^2 f\cos\alpha\sin\alpha + (1+e\cos f)[\cos^2\alpha - \sin^2\alpha]\cos\delta = 0$$

$$2e^2\sin^2 f\tan\alpha + (1+e\cos f)[1-\tan^2\alpha]\cos\delta = 0$$

$$(1+e\cos f)\cos\delta\tan^2\alpha + 2e^2\sin^2 f\tan\alpha + (1+e\cos f)\cos\delta = 0 \quad (31)$$

Which has the solution of quadratic equations

$$(\tan\alpha^*)_a = \frac{-2e^2\sin^2 f \pm \sqrt{4e^4\sin^4 f - 4(1+e\cos f)^2\cos^2\delta}}{2(1+e\cos f)\cos\delta} \quad (32)$$

This equation represents the control law that maximizes the rate of change of semi-major axis. It computes the actual sail pitch/cone angle profile necessary to increase the semi-major axis at a maximum rate.

Optimal control law for the rate of change of eccentricity

As previous, we observe that the required direction to maximize certain variable is given by $\tan\tilde{\alpha} = \frac{1+e\cos f}{e\sin f} = \frac{p/r}{e\sin f}$, which represents the transverse component divided by the radial component of the primer vector. Thus, in case of eccentricity, setting

$$\tan\tilde{\alpha} = \frac{\Xi_t^e}{\Xi_s^e} = \frac{\cos f + \frac{r}{p}(e+\cos f)}{\sin f} = \frac{(2+e\cos f)\cot f}{(1+e\cos f)} + \frac{e\csc f}{(1+e\cos f)} \quad (33)$$

The maximum rate of change of the orbital eccentricity follows directly as (Figs. 3.1 and 3.2);

$$(\tan\alpha^*)_e = \frac{-2e^2\sin^2 f \pm \sqrt{4e^4\sin^4 f - 4\left(\frac{(2+e\cos f)\cot f + e\csc f}{(1+e\cos f)}\right)^2\cos^2\delta}}{2\left(\frac{(2+e\cos f)\cot f + e\csc f}{(1+e\cos f)}\right)\cos\delta} \quad (34)$$

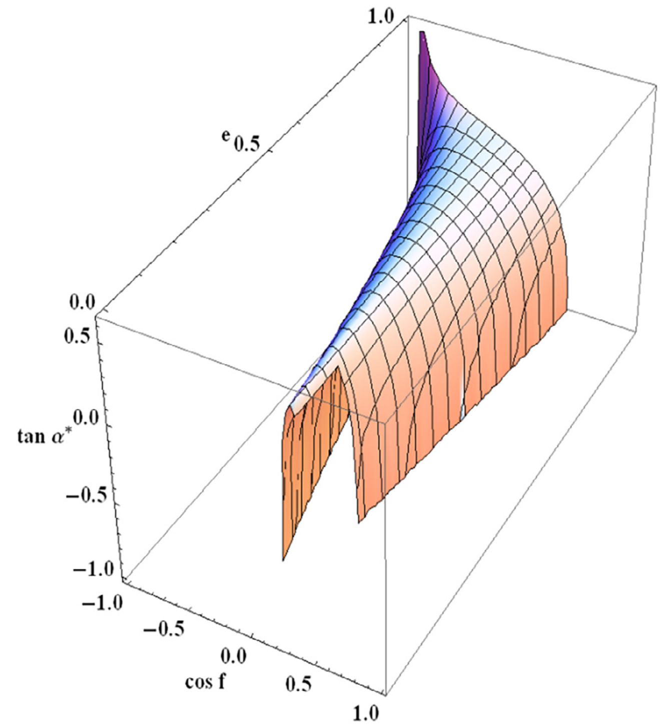

Fig. 3.1. The optimum cone angle that maximize the rate of change of eccentricity when taking the positive sign in the numerator.

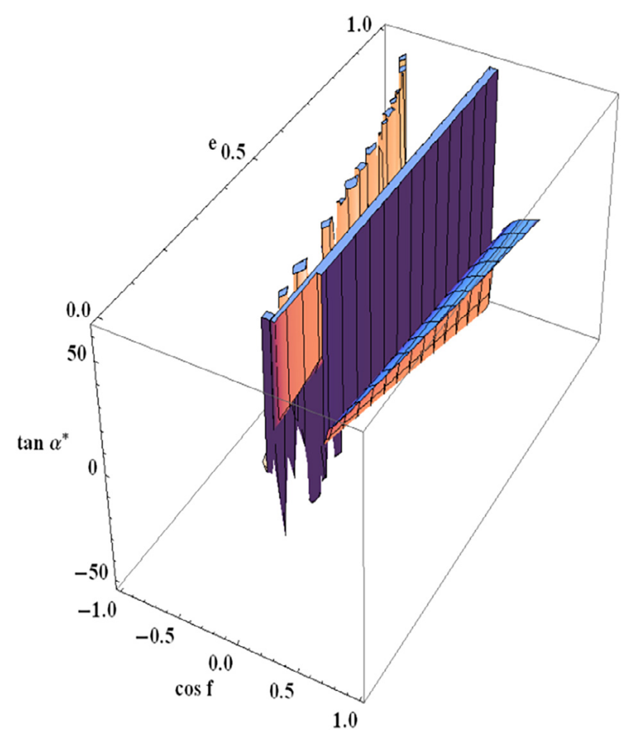

Fig. 3.2. The optimum cone angle that maximize the rate of change of eccentricity when taking the negative sign in the numerator.

Optimal control law for the rate of change of inclination

Changes in the out-of-plane orbital elements, such as inclination and right ascension of the ascending node, can be effected by the use of simple switching functions. For maximum rate of change of inclination, the solar sail thrust can be directed alternately above and below the orbit plane every half-orbit, by the *sign* function which has +1 or −1. In what follows we will find an optimum cone angle that maximize the rate of change of inclination

$$\frac{\partial}{\partial\alpha}\left(\frac{di}{df}\right)=\frac{r^3}{\mu p}sign\left[\cos(f+\omega)\right]\frac{\partial}{\partial\alpha}W=0$$

From which one can obtain

$$=-\frac{r_g^2 L_s r^3}{4c^2\mu p}\sqrt{\frac{GM_s}{R^5}}\,sign\left[\cos(f+\omega)\right](\cos^2\alpha-\sin^2\alpha)\sin\delta=0$$

Which has the solution

$$(\cos^2\alpha-\sin^2\alpha)=0,\quad\Rightarrow\quad(\tan\alpha^*)_i=1\quad\Rightarrow\quad\alpha_i^*=45^\circ \tag{35}$$

This optimal angle is 45°, enables us to maximize angular momentum.

If we substitute the control law into the inclination equation in Lagrange planetary equations, and integrate over one orbit, using the average over the true anomaly $\langle\cdot\rangle_f$, we can obtain the change in inclination per one orbit as (Fig. 4);

$$W_{\alpha=45^\circ}=-\frac{r^2L_s}{8c^2}\sqrt{\frac{GM_s}{R^5}}\sin\delta$$

$$\left\langle\frac{di}{df}\right\rangle_f=-\frac{r_g^2L_s}{8c^2\mu p}\sqrt{\frac{GM_s}{R^5}}\sin\delta\langle r^3\cos(f+\omega)\rangle_f$$

$$\Delta i=-\frac{r_g^2L_s}{16\,c^2\mu p}\sqrt{\frac{GM_s}{R^5}}\sin\delta\cos\omega\frac{e}{(1-e^2)^{3/2}}\quad\text{(degrees per orbit)} \tag{36}$$

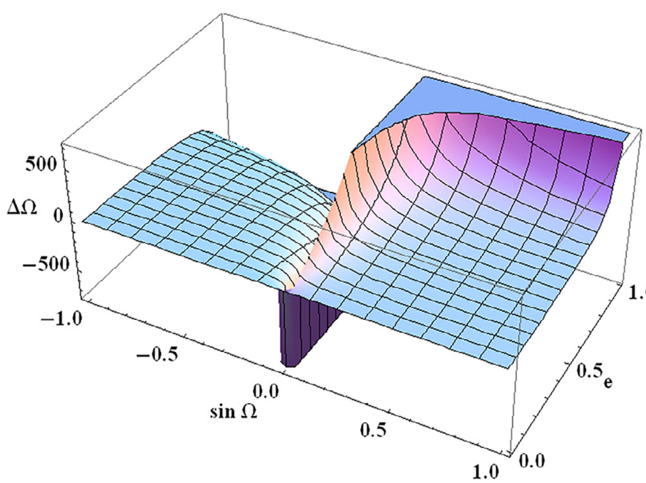

Fig. 4. The optimum change in the longitude in the ascending node ΔΩ versus the inclination sin$i$ and eccentricity.

Optimal control law for the rate of change of ascending node

The procedure is the same as in optimal control law for inclination

$$\frac{\partial}{\partial\alpha}\left(\frac{d\Omega}{df}\right)=\frac{r^3}{\mu p\sin i}sign\left[\sin(f+\omega)\right]\frac{\partial}{\partial\alpha}W=0 \tag{37}$$

Which has the same solutions as these maximizing the inclination and in good agreement with the previous results. If we substitute this control law into the ascending node in Lagrange planetary equations, and integrate over one orbit, we can obtain the change in ascending node per orbit. We find that the change in ascending node per orbit is independent of orbit radius and only depends on the sail lightness number as;

$$\Delta\Omega=-\frac{r_g^2L_s}{16c^2\mu p\sin i}\sqrt{\frac{GM_s}{R^5}}\sin\delta\sin\omega\frac{e}{(1-e^2)^{3/2}}\quad\text{(degrees per orbit)} \tag{38}$$

However, closer orbits to the Sun have shorter orbit periods, and so the time to achieve an overall inclination change is shorter.

Optimal control law for the rate of change of argument of perihelion

We observe that the required direction to maximize certain variable is given by $\tan\tilde{\alpha}=\frac{1+e\cos f}{e\sin f}=\frac{p/r}{e\sin f}$, which represents the transverse component divided by the radial component of the primer vector. Thus, in case of argument of perihelion, we obtain (Figs. 5.1 and 5.2)

$$\tan\tilde{\alpha}=\frac{\Xi_t^\omega}{\Xi_s^\omega}=\frac{(1+(r/p))\sin f}{\cos f}=(1+(r/p))\tan f=\left(\frac{2+e\cos f}{1+e\cos f}\right)\tan f$$

$$(\tan\alpha^*)_\omega=\frac{-2e^2\sin^2f\pm\sqrt{4e^4\sin^4f-4\left(\left(\frac{2+e\cos f}{1+e\cos f}\right)\tan f\right)^2\cos^2\delta}}{2\left(\left(\frac{2+e\cos f}{1+e\cos f}\right)\tan f\right)\cos\delta} \tag{39}$$

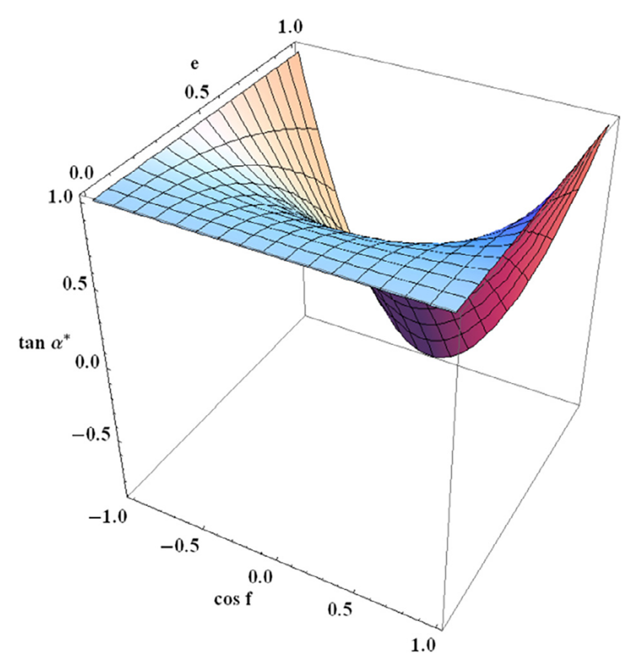

Fig. 5.1. The optimum cone angle that maximize the rate of change of argument of perihilion when taking the positive sign in the numerator.

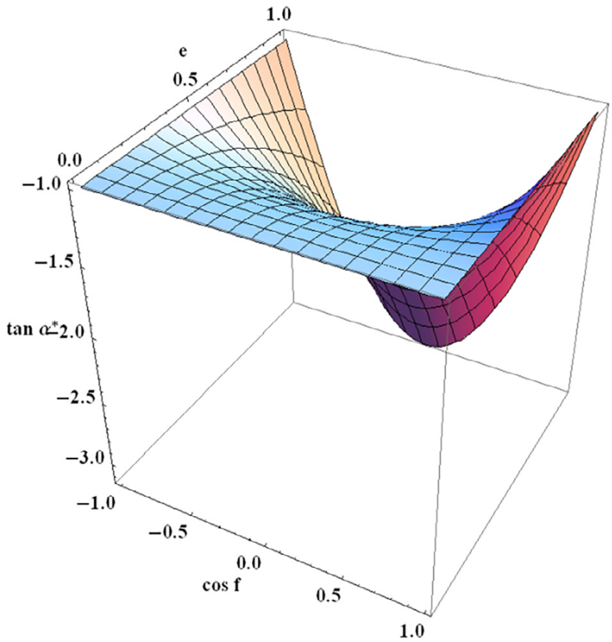

Fig. 5.2. The optimum cone angle that maximize the rate of change of argument of perihilion when taking the negative sign in the numerator.

Conclusion and future work

In the present work, we have studied the problem of solar sailing dynamics due to the Poynting–Robertson drag. The force model on the solar sail configurations is constructed. An optimum force vector due to Poynting–Robertson drag is obtained. Some analytical control laws with some mentioned input constraints for optimizing solar sail dynamics in heliocentric orbit using Lagrange's planetary equations are mathematically explored. Optimum force vector in a required direction is maximized by deriving optimal sail cone angle. New control laws that maximize thrust to obtain certain required maximization in some particular orbital element are obtained. The author in a forthcoming work will try to solve the problem again using the Lagrange multipliers and compare the results hopefully obtained with the results have been obtained in the current manuscript.

Appendix A. Supplementary data

Supplementary data associated with this article can be found, in the online version, at http://dx.doi.org/10.1016/j.rinp.2018.03.057.

References

[1] Tsiolkovsky KE. Extension of man into outer space. Cf. Also K. E. Tsiolkovskiy, Symposium on Jet Propulsion, No. 2, United Scientific and Technical Presses (NIT), 1936, (1921).
[2] Tsander K. (quoting a 1924 report by the author). From a scientific heritage. NASA Technical Translation TTF-541, 1967.
[3] Rizvi F. Solar Sail Attitude Dynamics and Coning Control: On Developing Control Methods for Solar Sail Coning at Orbit Rate to Attain Desired Orbital Effects. A M. Sc. thesis, Faculty of the Graduate School of the University of Colorado, Department of Aerospace Engineering Sciences, (2010).
[4] Wright JL. Space sailing. Gordon and Breach Science Publishers. Second printing 1993, 1992.
[5] Tsu TC. Interplanetary travel by solar sail. Am Rocket Soc J 1959;29:422–7.
[6] London HS. Some exact solutions of the equations of motion of a solar sail with constant sail setting. Am Rocket Soc J 1960;30:198–200.
[7] Zhukov AN, Lebedev VN. Variational problem of transfer between heliocentric orbits by means of a solar sail. Kosmicheskie Issledovaniya (Cosmic Research) 1964;2:45–50.
[8] Jayaraman TS. Time optimal orbit transfer trajectory for solar sail spacecraft. J Guidance Control 1980;3(6):536–42.
[9] Wood LJ, Bauer TP, Zondervan KP. Comment on time optimal orbit transfer trajectory for solar sail spacecraft. J Guidance Control Dyn 1982;5(2):221–4.
[10] Powers RB, Coverstone VL, Prussing JE. Solar sail optimal orbit transfers to synchronous orbits. In: Proceedings of the 1999 AAS/AIAA Astrodynamics; 1999.
[11] Powers RB, Coverstone VL. Optimal solar sail orbit transfers to synchronous orbits. J Astronaut Sci 2001;49(2):269–81. Specialist Conference, Girdwood, Alaska, volume 103 of Advances in the Astronautical Sciences. p. 523–38.
[12] Sauer CG. Optimum solar sail interplanetary trajectories. Paper presented at AIAA/AAS Astrodynamics Conference, San Diego, CA, AIAA Paper 76, 792; 1976.
[13] Hughes GW, McInnes CR. Solar sail hybrid trajectory optimization. In: Proceedings of the 2001 AAS/AIAA Astrodynamics Specialist Conference, Quebec City, Quebec, Canada, volume 109 of Advances in the Astronautical Sciences; 2001. p. 2369–80.
[14] Dachwald B. Solar Sail Performance Requirements for Missions to the Outer Solar System and Beyond. IAC-04-S.P. 11 55th International Astronautical Congress 2004 – Vancouver, Canada; 2004.
[15] Thomas JW, McInne R. Solar sail dynamics in the three-body problem: homoclinic paths of points and orbits. Int J Non-Linear Mech 2010. http://dx.doi.org/10.1016/j.ijnonlinmec.2008.01.001. Elsevier Publishers.
[16] Wie B. Solar sail attitude control and dynamics, Part 1. J Guidance Control Dyn 2004;27(4).
[17] Sheng-Ping G, Yun-Feng G, Li Jun-Feng. Solar sail time-optimal interplanetary transfer trajectory design. Res Astron Astrophys 2011;11(8):981–96.
[18] Abd El-Salam F.A. Some new locally optimal control laws for sailcraft dynamics in heliocentric orbits. Hindawi Publishing Corporation, Journal of Applied Mathematics, Volume 2013, Article ID 353056, 16 pages, http://dx.doi.org/10.1155/2013/353056, (2013).
[19] Kawaguchi J. A Solar Power Sail Mission for A Jovian Orbiter and Trojan Asteroid Flybys. COSPAR04-A-01655; 2004.
[20] Mori O, Sawada H, Hanaoka H, Kawaguchi J, Shirasawa Y, Sugita M, et al. Development of deployment system for small size solar sail mission. Trans Jpn Soc Aeronaut Space Sci Space Technol Jpn 2009;7(26). Pd_87-Pd_94.
[21] Tsuda Y, Mori O, Funase R, Sawada H, Yamamoto T, Saiki T, et al. Achievement of IKAROS – Japanese deep space solar sail demonstration mission. Acta Astronautica 2013;82:183–8.
[22] Spencer DA, Stetson DA, Betts B, Plante B, Foley JD, Bellardo JM. Testing the lightsail program: advancing solar sailing technology using a cubesat platform. JoSS 2016;5(2):531–50.
[23] Betts B, Nye B, Vaughn J, Greeson E, Chute R, Spencer D, et al. LightSail1 Mission Results and Public Outreach Strategies. Paper presented at Fourth International Symposium on Solar Sailing 2017, Kyoto, Japan; 2017.
[24] Betts B, Spencer D, Nye B, Munakata R, Bellardo J, Wong S, et al. LightSail2: controlled Solar Sailing Using a CubeSat. Paper presented at Fourth International Symposium on Solar Sailing 2017, Kyoto, Japan; 2017.
[25] Hilverda M, Davis J. Communicating LightSail: embedded Reporting and Web Strategies for Citizen-Funded Space Missions. Poster session presented at the American Geophysical Union Fall Meeting 2015 San Francisco CA; 2015.
[26] Plante B, Spencer D, Betts B, Chait S, Bellardo J, Diaz A, et al. LightSail2 ADCS: from Simulation to Mission Readiness. Paper presented at Fourth International Symposium on Solar Sailing 2017, Kyoto, Japan; 2017.
[27] Poynting JH. Phil Trans Roy Soc 1903;A202:525, reprinted with corrections in his Collected Scientific papers (1920) p. 304, (1903).
[28] Robertson HP. Dynamical effects of radiation in the solar system. Monthly Notices of the Royal Astronomical Society (Royal Astronomical Society) 97: 423–8. Bibcode:1937 MNRAS..97..423R; 1937.
[29] Klacka J, Petrzala J, Pastor P, Komar L. The Poynting-Robertson effect: a critical perspective. Icarus 2014;232:249. http://dx.doi.org/10.1016/j.icarus.2012.06.044.
[30] Abraham M. Ann. Phys. 1903;10:105–79. See page 156.
[31] Dirac PAM. Proc Roy Soc Lon A 1938;167:148–69. Eq. (24).
[32] Pauli W. Theory of relativity. New York: Dover Pubs, Inc.; 1958. p. 99 and p. 139.
[33] Lorentz HA. The theory of electrons. New York: Dover Pubs, Inc.; 1904. reprinted 1915, (1952).